Graphane

DOI: 10.1002/anie.201206799

On the Way to Graphane—Pronounced Fluorescence of Polyhydrogenated Graphene**

*Ricarda A. Schäfer, Jan M. Englert, Peter Wehrfritz, Walter Bauer, Frank Hauke, Thomas Seyller, and Andreas Hirsch**

Although graphene and its unprecedented physical properties were discovered some time ago,[1] first concepts on the chemical functionalization of the unreactive perfect graphene basal planes have been developed only recently.[2–7] Increasing the solubility of graphene and combining its properties with those of other compound classes is of major interest. Another objective is the exploration of its intrinsic chemical reactivity and the synthesis of functional derivatives. In this regard, graphane, a fully hydrogenated graphene scaffold, represents a fundamental synthetic target. Theoretical studies on graphane were published in 2007 by Sofo et al.[8] They demonstrated that the two energetically most favorable types of graphane consist of fused cyclohexane rings with either boat or chair configurations (Figure 1). The more stable chair configuration avoids CH staggering completely. Graphane is predicted to be an insulator with a band gap of 3.5 eV for the chair and 3.7 eV for the boat configuration. In computational studies on plausible hydrogenation mechanisms[9] it was suggested that the deformation induced by the hydrogen addition to the sp^2-hybridized lattice atoms leads to increased reactivity in close proximity to these new $C_{sp^3}H$ centers, hence favoring an "island-type" hydrogenation. In contrast to fullerenes and carbon nanotubes, addition reactions to graphene can take place at both sides of the carbon network. This can lead to strain-free configurations, which also explains the unexpected high reactivity of graphene we observed recently in arylation and alkylation reactions.[2,10]

So far no wet-chemical approaches have been reported for the hydrogenation of graphene. A few other approaches have been described,[13–15] including graphene hydrogenation by plasma.[11,12] Based on work by Billups et al.[16] we have recently reported on the wet-chemical arylation and alkylation of graphene using graphite intercalation compounds (GICs) as activated starting materials.[2,10] Here, the chemical functionalization is accompanied by an efficient exfoliation and individualization of the graphene sheets. Using our experience in reductive graphene chemistry we describe herein a Birch-type reaction sequence[17] to generate polyhydrogenated graphene (phG). The Birch reduction is widely used for hydrogenation of polyaromatic hydrocarbons (PAHs) and carbon allotropes.[18–20] The efficiency of the Birch reaction as a possible route towards phG was evaluated with a series of proton sources, namely, methanol, ethanol, propan-2-ol, *tert*-butyl alcohol, and water in combination with alkali metals as reducing agents. We found the highest hydrogenation efficiency for lithium and water. The resulting polyhydrogenated products are characterized by a pronounced but not exhaustive H-addition. Significantly, these phGs display strong fluorescence stemming from the remaining π-conjugated regions within isolated and electronically decoupled carbon sheets.

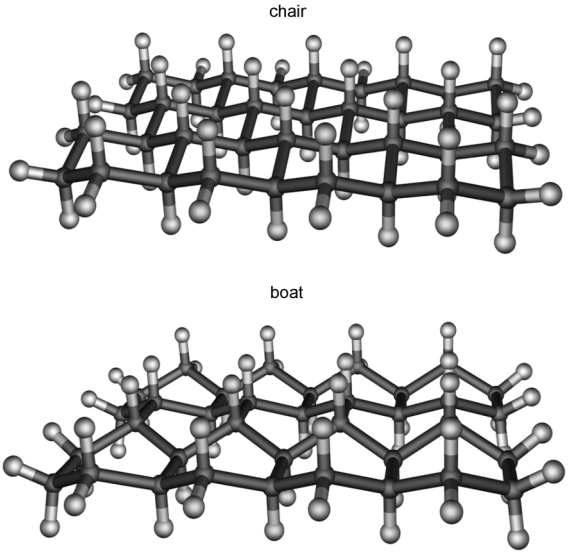

Figure 1. Chair and boat configurations of graphane.

In the first reaction step, 1 equiv of spherical graphite flakes were intercalated with a fivefold excess of lithium metal in liquid ammonia at −78 °C for two hours (Scheme 1). After the addition of 10 equiv of deionized water to the reaction mixture, the ammonia evaporated as the mixture was allowed to warm to room temperature. The remaining solid was suspended in an ethanol/water (1:1) mixture and subsequently transferred to a separation funnel and washed with cyclohexane/water, and then filtered through a fleece-rein-

[*] R. A. Schäfer, J. M. Englert, W. Bauer, F. Hauke, A. Hirsch
Department of Chemistry and Pharmacy
and Institute of Advanced Materials and Processes (ZMP)
University of Erlangen-Nuremberg
Henkestrasse 42, 91054 Erlangen (Germany)
E-mail: andreas.hirsch@chemie.uni-erlangen.de
P. Wehrfritz, T. Seyller
Department of Physics, University of Erlangen-Nuremberg
Erwin-Rommel-Strasse 1, 91058 Erlangen (Germany)

[**] We thank the Deutsche Forschungsgemeinschaft (SFB 953, Project A1 "Synthetic Carbon Allotropes"), the Interdisciplinary Center for Molecular Materials, the European Research Council (grant 246622 GRAPHENOCHEM), and the Graduate School Molecular Science financial support and Christian Krechel (WW1, M. Göken) for SEM measurements.

Supporting information for this article is available on the WWW under http://dx.doi.org/10.1002/anie.201206799.

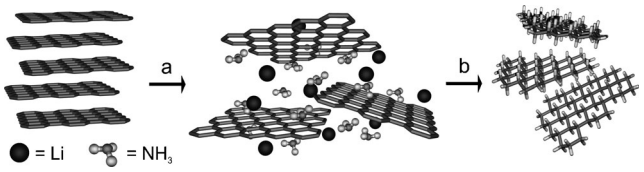

Scheme 1. Birch-type wet-chemical hydrogenation or deuteration of graphene, which was prepared from graphite with isotopically pure solvents and quenching reagents: a) NH_3/ND_3, Li, 2 h; b) H_2O/D_2O.

forced cellulose membrane (200 nm pore size). Surprisingly, the alkalide solution retained its reducing activity after the addition of water as indicated by the persistence of the blue color. Also, since only little gas evolution was detected before the evaporation of the ammonia, it can be concluded that no significant H_2 formation took place at that stage. After the product had dried, its characteristic brown/golden color remains which we take as strong evidence for the extensive covalent hydrogen functionalization and extensive rupture of the π conjugation.

Two reaction mechanisms can be considered for this hydrogenation sequence. One possibility would be the protonation of the negatively charged graphene sheets. This process would require a pronounced basicity or nucleophilicity of the graphenide intermediates. Because the negative charge is expected to be delocalized, this requirement does not seem to be met. An alternative would be a single-electron transfer from the graphenide sheets to the water molecules forming H radicals. Subsequent radical recombination reactions would lead to either the formation of molecular hydrogen or the hydrogenation of graphene. The first mechanism seems more reasonable for small aromatic molecules where the charge is localized and delocalization does not play a significant role. In the present case we favor the second mechanism which includes H radical species that are suspected to be highly reactive even towards neutral or charged graphite surfaces.[16,21] An analogous mechanism is probably also operative during the arylation[2] and alkylation[10] of graphenides with electrophiles which we reported recently.

These considerations provide an explanation of why water is more efficient in our graphene hydrogenation than the alcohol-based proton sources commonly used in Birch reductions. Upon the addition of H_2O to the liquid ammonia (−78 °C) most of the water is almost instantaneously removed from the reaction mixture by the formation of ice as well as ammonium hydroxide. When the cooling bath is removed, the temperature of the reaction mixture increases to the boiling point of ammonia. As a consequence NH_3 is removed from the ammonia/water⇌ammonium hydroxide equilibrium and water is slowly released. This guarantees the presence of a low local concentration of hydrogen favoring the hydrogenation of graphene rather than the recombination to H_2.

Thermogravimetric analysis coupled with mass spectrometry (TGA-MS) provided important information about the composition of the hydrogenation product. For this purpose, both the functionalized product and the starting material were heated at 700 °C under a constant flow of helium. The major mass loss took place at 400–600 °C, where an intensive MS signal for molecular hydrogen ($m/z = 2$) was detected (Figure 2). Signals at $m/z = 17$ and 18 were also detected at higher temperatures (see Figure S1 in the Supporting Information), which can be assigned to hydroxide and water

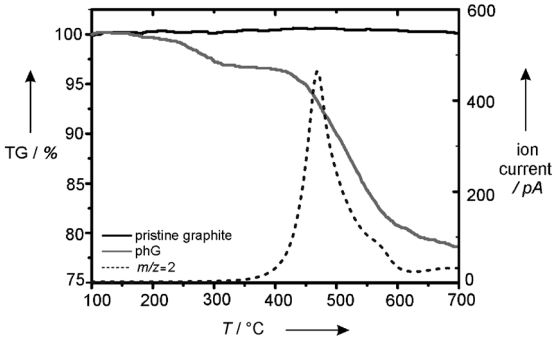

Figure 2. Thermogravimetric analysis coupled with mass spectrometry of polyhydrogenated graphene (phG); black, gray: TG traces; dotted black line: ion current of $m/z = 2$ [H_2].

formed by the decomposition of trapped LiOH during the formation of Li_2O. No other cations except from atmospheric gases were detected in the range of $m/z = 10$ to 300. In reductions with *t*BuOH as the hydrogen source, the hydrogen signal was considerably weaker. As further proof of graphene hydrogenation we prepared also deuterated samples, as outlined in detail in the Supporting Information. To detect the $m/z = 4$ signal of D_2, the material was heated under a constant flow of nitrogen instead of helium, which would yield an $m/z = 4$ signal as well. A two-step mass loss was observed by thermogravimetry. The first mass loss at 200–300 °C can be attributed to $m/z = 18$, 19, and 20 in the ion current derived from the cleavage of deuterated amines (-NHD or $-ND_2$) or deutroxyl (-OD) functional groups. The second step can be traced back to the removal of D_2 and smaller amounts of HD which were detected as $m/z = 3$ and 4, respectively (see Figure S2 in the Supporting Information).

Raman spectroscopy has turned out to be a very powerful method for the investigation of covalently functionalized carbon nanotubes and graphene. The Raman spectrum of a bulk sample of our highly hydrogenated graphene material measured at $\lambda_{exc} = 532$ nm exhibited two very broad bands between 1000 and 3000 cm^{-1} covering the complete D-, G-, and 2D-band regions. Unlike Raman spectra of graphene and functionalized graphene including highly defective graphene oxide, there were no indications for the presence of D- or G-band features. Thus, no information about the stacking sequence, layer decoupling, doping level, defect density, or strain could be obtained from these spectra (Figure 3).

To prove the carbonaceous nature of the reaction product, we conducted temperature-induced defunctionalization inside the spectrometer. It appears that the intensities of the broad bands decrease with increasing temperature and that the D and G bands recover at temperatures higher than 300 °C. The mean spectrum at 500 °C exhibited the typical Raman features reported for highly functionalized graphene with an I_D/I_G ratio of approximately 1.1. This type of spectrum

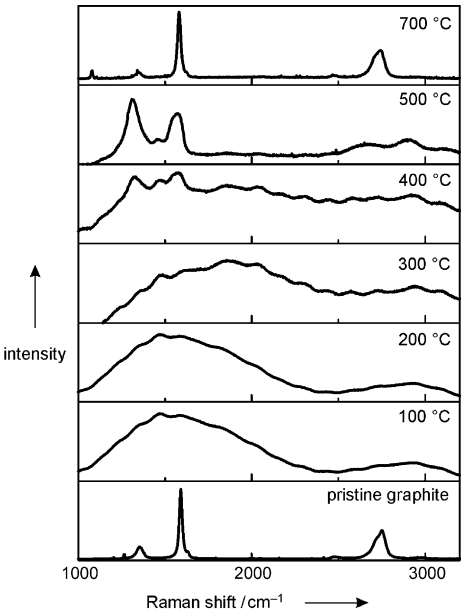

Figure 3. Mean Raman spectra of pristine graphite (starting material, bottom), polyhydrogenated graphene at different temperatures, and the defunctionalized material after TGA measurement (top).

is expected for carbonaceous materials with mean point defect distances below 2 nm.[22] The 2D band is broadened and accompanied by a D + G′ band at 2900 cm^{-1}. After the sample was heated further to 700 °C (TG treatment) complete conversion into graphite took place and the spectrum of the starting material was recovered. This behavior can be explained by temperature-induced dehydrogenation.

The hydrogenation was further verified by solid-state CP-MAS ^{13}C NMR spectroscopy (CP-MAS = cross-polarization magic-angle spinning), and signals at 223.2, 177.4, 130.6, 85.6, and 44.3 ppm were observed (Figure S3 in the Supporting Information). The peak at 130 ppm can be assigned to the $^{13}C_{sp^2}$ atoms and the high-intensity upfield signal at 44.3 ppm can be traced back to the $C_{sp^3}H$ centers.

The IR spectra of the deuterated and the hydrogenated samples were compared. The IR spectrum of the hydrogenated sample (Figure 4) shows two sharp bands at 3676 and 3566 cm^{-1}, which can be assigned to free hydroxyl and amino groups introduced in side reactions, and a broad signal at 2852 cm^{-1} which is characteristic for CH vibrations. All these bands are shifted to lower wavenumbers for the deuterated sample on account of the isotope effect and appear now at 2708 and 2629 cm^{-1} (OD and ND vibrations) and 2135 cm^{-1} (CD vibrations). In the region between 1500 and 500 cm^{-1}, characteristic for C–C vibrations, no such changes were detected.

The hydrogenated material was further investigated by X-ray photoelectron spectroscopy (XPS). In accordance with the insulating nature of the material, a strong shift of the core levels was observed which results from the charging of the sample during the measurement. In order to minimize this charging we used an electron flood gun for compensation. The survey spectrum of the sample (see Figure S4 in the Supporting Information) indicates that it consists of 69.0 % carbon,

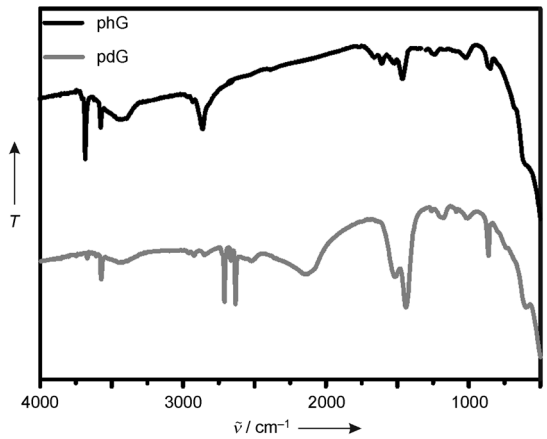

Figure 4. IR spectra of polyhydrogenated graphene (phG) and polydeuterated graphene (pdG).

18.8 % oxygen, 11.7 % lithium, and 0.5 % nitrogen. Note that hydrogen cannot be detected by XPS. The oxygen can be attributed primarily to the presence of LiOH. The small amount of nitrogen is either covalently attached or belongs to adsorbed residues of the ammonia. The C 1s line exhibits a shoulder which indicates the presence of two differently bonded carbon species. Further statements about exact bond types are impossible because of strong peak broadening due to residual differential charging.

The polyhydrogenated graphene was also investigated by atomic force microscopy. In the height profiles (Figure 5 b,c) extracted from the topography images monolayer steps with heights of 1 to 2 nm were determined. The center of the flake exhibited a height of 1 to 10 nm which can be a result of reaggregation, incomplete exfoliation, or folding of the functionalized material.

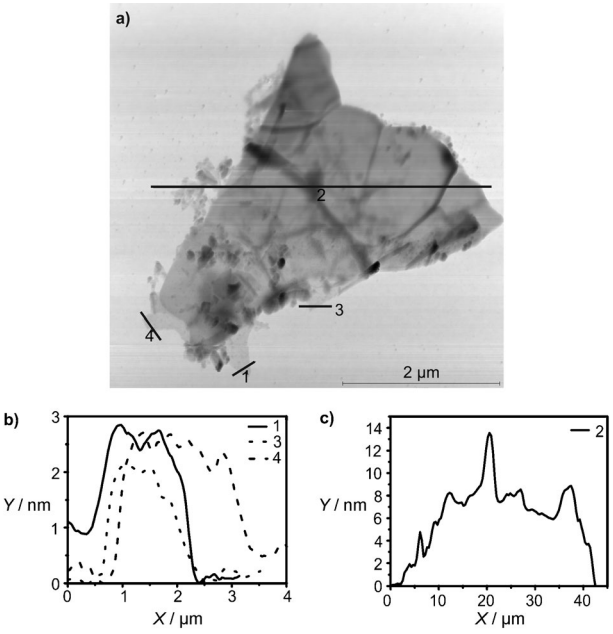

Figure 5. a) AFM image of (phG); b,c) height profiles of the paths labeled 1–4 in (a).

The brown/yellow color and the observed fluorescence of phG can be explained by the presence of a band gap and the change in the electronic properties generated by the high degree of functionalization. Upon excitation of phG with a conventional portable UV lamp ($\lambda_{exc} = 366$ nm), bright yellow emission can be seen (Figure 6c). This allowed for the convenient characterization by solid-state fluorescence spectroscopy. A broad emission in the visible spectrum spreading from 450 nm to 650 nm is observed upon excitation above 280 nm (Figure 6a). The broad spectrum indicates the presence of a variety of isolated and randomly sized nanographene domains that all contribute independently to the fluorescence intensity.

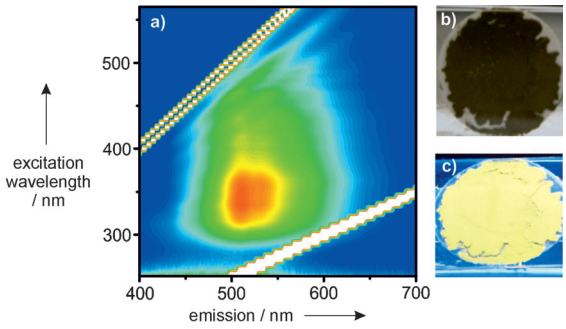

Figure 6. a) Emission/excitation map of phG (with increasing intensity from blue to red). Images of filtered phG b) before and c) during excitation with a handheld UV lamp ($\lambda_{exc} = 366$ nm).

In conclusion, we have presented the first wet-chemical synthesis of a highly hydrogenated graphene using a Birch-type reduction sequence. The key point for the efficient hydrogenation is the use of water as the hydrogen source, which under the applied reaction conditions is released very slowly causing the hydrogenation of graphene to be preferred over the competing H_2 formation. The hydrogenation is accompanied by a very strong fluorescence of the reaction product. This phenomenon demonstrates that during hydrogenation, isolated and electronically decoupled domains of π-conjugated regions are formed. Besides fundamental insights into graphene chemistry, a further implication of this study is that graphite can be used as convenient starting material for the wet-chemical preparation of graphene derivatives with remarkable optoelectronic properties. We are currently evaluating the extent to which these interesting properties can be fine-tuned by a systematic variation of the reaction conditions and also studying the fundamental nature of the photoluminescence.

Received: August 22, 2012
Published online: November 26, 2012

Keywords: carbon allotropes · fluorescence · graphane · graphene · hydrogenation

[1] K. S. Novoselov, A. K. Geim, S. V. Morozov, D. Jiang, Y. Zhang, S. V. Dubonos, I. V. Grigorieva, A. A. Firsov, *Science* **2004**, *306*, 666 – 669.
[2] J. M. Englert, C. Dotzer, G. Yang, M. Schmid, C. Papp, J. M. Gottfried, H.-P. Steinrück, E. Spiecker, F. Hauke, A. Hirsch, *Nat. Chem.* **2011**, *3*, 279 – 286.
[3] Z. Sun, D. K. James, J. M. Tour, *J. Phys. Chem. Lett.* **2011**, *2*, 2425 – 2432.
[4] Z. Jin, T. P. McNicholas, C.-J. Shih, Q. H. Wang, G. L. C. Paulus, A. J. Hilmer, S. Shimizu, M. S. Strano, *Chem. Mater.* **2011**, *23*, 3362 – 3370.
[5] E. Bekyarova, S. Sarkar, S. Niyogi, M. E. Itkis, R. C. Haddon, *J. Phys. D* **2012**, *45*, 154009.
[6] J. Malig, J. M. Englert, A. Hirsch, D. Guldi, *ECS Interface* **2011**, *20*, 53 – 56.
[7] A. Hirsch, J. M. Englert, F. Hauke, *Acc. Chem. Res.* **2012**, DOI: 10.1021/ar300116q.
[8] J. O. Sofo, A. S. Chaudhari, G. D. Barber, *Phys. Rev. B* **2007**, *75*, 153401.
[9] M. Z. S. Flores, P. A. S. Autreto, S. B. Legoas, D. S. Galvao, *Nanotechnology* **2009**, *20*, 465704.
[10] J. M. Englert, K. C. Knirsch, C. Dotzer, B. Butz, F. Hauke, E. Spiecker, A. Hirsch, *Chem. Commun.* **2012**, *48*, 5025 – 5027.
[11] D. C. Elias, R. R. Nair, T. M. G. Mohiuddin, S. V. Morozov, P. Blake, M. P. Halsall, A. C. Ferrari, D. W. Boukhvalov, M. I. Katsnelson, A. K. Geim, K. S. Novoselov, *Science* **2009**, *323*, 610 – 613.
[12] R. Balog, B. Jørgensen, J. Wells, E. Lægsgaard, P. Hofmann, F. Besenbacher, L. Hornekær, *J. Am. Chem. Soc.* **2009**, *131*, 8744 – 8745.
[13] S. Ryu, M. Y. Han, J. Maultzsch, T. F. Heinz, P. Kim, M. L. Steigerwald, L. E. Brus, *Nano Lett.* **2008**, *8*, 4597 – 4602.
[14] N. P. Guisinger, G. M. Rutter, J. N. Crain, P. N. First, J. A. Stroscio, *Nano Lett.* **2009**, *9*, 1462 – 1466.
[15] Y. Wang, X. Xu, J. Lu, M. Lin, Q. Bao, B. Özyilmaz, K. P. Loh, *ACS Nano* **2010**, *4*, 6146 – 6152.
[16] S. Chakraborty, J. Chattopadhyay, W. Guo, W. E. Billups, *Angew. Chem.* **2007**, *119*, 4570 – 4572; *Angew. Chem. Int. Ed.* **2007**, *46*, 4486 – 4488.
[17] A. J. Birch, *J. Chem. Soc.* **1944**, 430 – 436.
[18] Y. Vasil'ev, D. Wallis, M. Nuchter, B. Ondruschka, A. Lobach, T. Drewello, *Chem. Commun.* **2000**, 1233 – 1234.
[19] S. Pekker, J. P. Salvetat, E. Jakab, J. M. Bonard, L. Forró, *J. Phys. Chem. B* **2001**, *105*, 7938 – 7943.
[20] K. S. Subrahmanyam, P. Kumar, U. Maitra, A. Govindaraj, K. P. S. S. Hembram, U. V. Waghmare, C. N. R. Rao, *Proc. Natl. Acad. Sci. USA* **2011**, *108*, 2674 – 2677.
[21] H. P. Boehm, *Carbon* **2012**, *50*, 3154 – 3157.
[22] L. G. Cançado, A. Jorio, E. H. M. Ferreira, F. Stavale, C. A. Achete, R. B. Capaz, M. V. O. Moutinho, A. Lombardo, T. S. Kulmala, A. C. Ferrari, *Nano Lett.* **2011**, *11*, 3190 – 3196.

